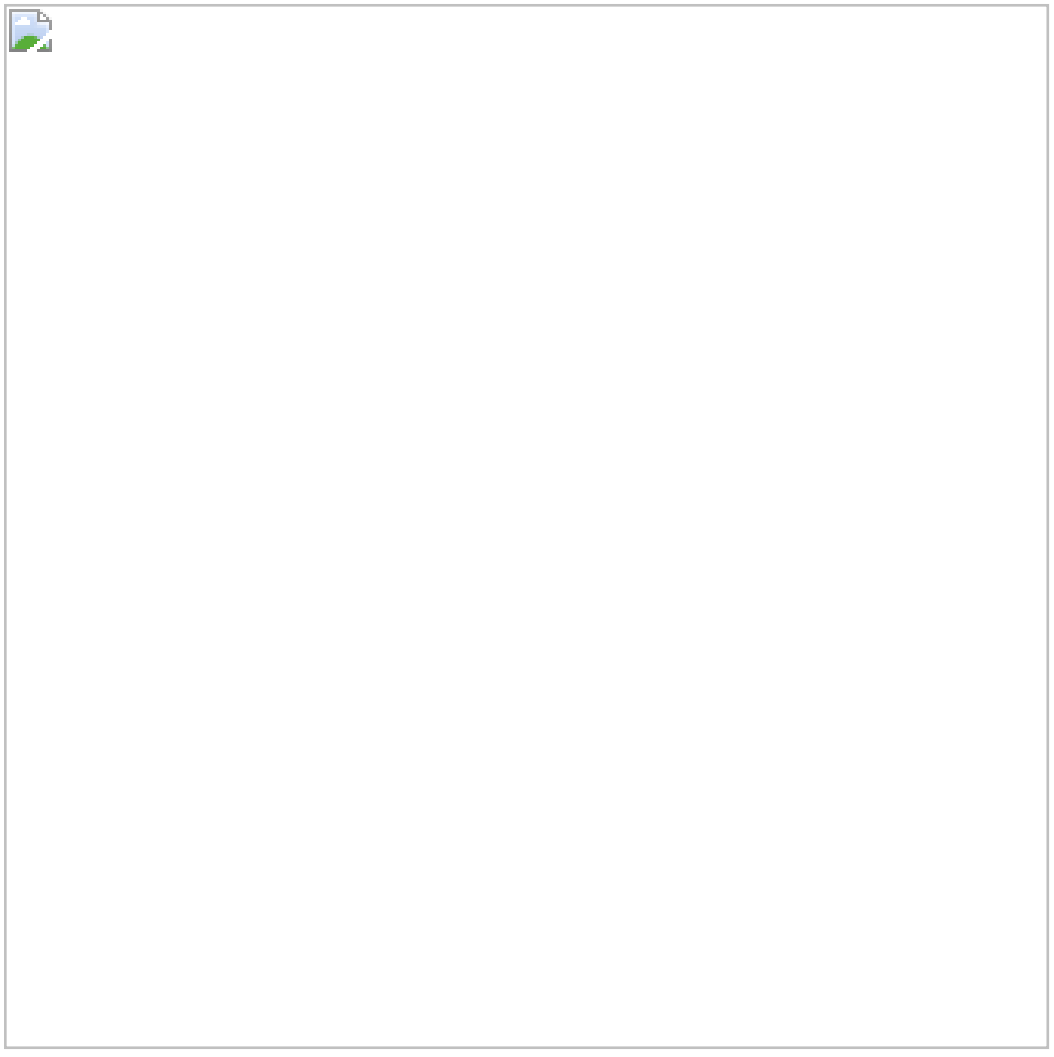

Sex Pheromone Gland of the Female European Corn Borer Moth, Ostrinia nubilalis (Lepidoptera, Pyralidae): Ultrastructural and Biochemical Evidences

Authors: Ma, Peter W. K., and Roelofs, Wendel L.

Source: Zoological Science, 19(5) : 501-511

Published By: Zoological Society of Japan

URL: https://doi.org/10.2108/zsj.19.501

ZOOLOGICAL SCIENCE **19**: 501–511 (2002)

Sex Pheromone Gland of the Female European Corn Borer Moth, *Ostrinia nubilalis* (Lepidoptera, Pyralidae): Ultrastructural and Biochemical Evidences

Peter W. K. Ma[1*] and Wendel L. Roelofs[2]

[1]*Department of Entomology and Plant Pathology, Mississippi State University, Mississippi State, MS 39762 U.S.A.*
[2]*Department of Entomology, NYS Agricultural Experiment Station, Cornell University, Geneva, NY 14456, U.S.A.*

ABSTRACT—The sex pheromone gland of the female European corn borer moth, *Ostrinia nubilalis* was studied using light and electron microscopy. The pheromone gland is formed by hypertrophied epidermal cells at the mid-dorsal region of the intersegmental membrane between abdominal segments 8 and 9/10. Active glandular cells contain extensive apical membrane foldings, a single nucleus, many free ribosomes, numerous mitochondria, microtubules and lipid droplets. Smooth endoplasmic reticulum is scanty. In young moths, the glandular cells are smaller in size, the microvilli at the apical membrane are poorly developed and the cytoplasm contains fewer mitochondria, microtubules, and no lipid droplets. The surrounding unmodified epidermal cells are small cuboidal or squamous cells. These cells have ill-defined apical membrane foldings and do not contain lipid droplets in the cytoplasm and the overlying cuticle. Fatty acids analyses revealed the presence of the sex pheromone components, *(E)*-11-tetradecenyl acetate, and their immediate precursors, methyl *(E)*-11- and methyl *(Z)*-11-tetradecenoate, only in the dorsal portion of the cylindrical intersegmental membrane. Results of the present study show that the sex pheromone gland of *O. nubilalis* is restricted to the dorsal aspect of the intersegmental membrane between segments 8–9/10 and is not a ring-gland.

Key words: gas chromatography, intersegmental membrane, SEM, TEM

INTRODUCTION

Sex pheromone glands of female Lepidoptera are commonly found as modified intersegmental membranes between the 8th and 9th abdominal segments (Götz 1951; Percy-Cunningham and MacDonald 1987). They also occur between abdominal segments 7 and 8 in *Sesamia nonagrioides* (Noctuidae) (Sreng and Sreng 1988), around the ostium bursae in *Plutella xylostella* (Plutellidae) (Chow *et al*. 1976), and at the papillae anales in *Heliothis virescens* Fabricius (Teal *et al.* 1983). In general, the modified intersegmental membrane is lined with a glandular epidermis made up of hypertrophied cells. However, the location of the hypertrophied cells on the modified intersegmental membrane varies considerably among different moth species (Percy-Cunningham and MacDonald 1987).

The European corn borer, *Ostrinia nubilalis*, is a serious agricultural pest in many parts of the world including the United States. Female *O. nubilalis* uses a mixture of *(Z)* -11- and *(E)* -11-tetradecenyl acetate (Z/E11-14:OAc) as their sex pheromone (Klun 1968; Klun and Junk 1970; Kochansky *et al.* 1975). Using light microscopy, Hammad (1961) reported that the entire intersegmental membrane between the 8th and 9th abdominal segments in female *O. nubilalis* is modified to form the ring-like sex pheromone gland, with the ventral cells being much larger than those located dorsally.

Sex pheromone production in female *O. nubilalis* is regulated by PBAN (pheromone biosynthesis activating neuropeptide)-like factors (Ma and Roelofs 1995). Information on how the PBAN-like factors might affect the ultrastructure of the sex pheromone gland is necessary for a future understanding of the action of the PBAN-like factors. To date, ultrastructural information on the sex pheromone gland of *O.nubilalis* is lacking.

In the present study, light and electron microscopical studies are conducted to describe the ultrastructural features of the sex pheromone gland of *O. nubilalis*. In addition,

* Corresponding author: Tel. +1-662-325-2978;
FAX. +1-662-325-8837.
E-mail: pma@entomology.msstate.edu

gas chromatographic analysis is used to localize the distribution of the sex pheromone, E/Z11-14:OAc, and its biosynthetic acid intermediates in the intersegmental membrane between abdominal segments 8 and 9/10 to confirm the exact location of the sex pheromone gland of *O. nubilalis*.

MATERIALS AND METHODS

Insects

Pupae were obtained from a culture maintained at the New York State Agricultural Experiment Station at Geneva, New York. They were sexed and adults that emerged were held separately in 3.8 l jars. Pupae and adults were kept at 25±1°C under a 16:8 (L:D) photoperiod with ca. 70% humidity provided by a wet paper towel hung inside the jars. All insects used in this study were of the bivoltine *E* strain that produces a sex pheromone blend containing 99% E and 1% Z isomer of 11–14:OAc (Glover *et al.* 1987).

Tissue preparation

Ovipositors (abdominal segments 8-10) were extruded by applying slight pressure on the abdomens of the moths and were excised using a razor blade. For light and scanning electron microscopy, the entire ovipositor was immersed in fixative. For transmission electron microscopy, the ovipositors were placed in a drop of a modified Weever's insect saline (Carrow *et al.* 1981) and the intersegmental membrane between abdominal segments 8 and 9/10 was then dissected out under the saline and placed immediately in fixative.

Routine fixation was accomplished by immersing the tissues directly into 4% glutaraldehyde in 0.1M phosphate buffer (pH 7.4) at 4°C for 24 hr. For scanning and transmission electron microscopy, tissues were postfixed in 1% OsO_4 in 0.1M phosphate buffer for 8 hr at room temperature. After fixation, all tissues were rinsed with 0.1 M phosphate buffer and dehydrated by passing through a graded series of ethanol.

Light Microscopy

Dehydrated tissues were passed through a few changes of xylenes and embedded in Paraplast ® (56°C m.p. Fisher Scientific). Sections were cut at 6 μm, stained with hematoxylin and eosin and mounted in Permount® (Fisher Scientific).

Scanning electron microscopy

Dehydrated ovipositors were soaked in three changes of pentane and allowed to air dry in a fume hood (G.T.Baker, personal communication). Dried specimens were mounted on aluminum stubs using double sticky tape, sputter coated with gold-palladium and then examined under a Hitachi S-530 scanning electron microscope at 15 kV.

Transmission electron microscopy

After dehydration, tissues were placed in 1:2, 1:1 and 2:1 Spurr:ethanol. They were then infiltrated with five changes of Spurr resin of 6 hr each and finally embedded in the same at 60°C for 24 hr. Thick sections (1/2–1 μm) were stained with toluidine blue. Thin sections (showing silver interference color) were cut using glass knives and collected on Formvar-coated copper slot grids. After staining with uranyl acetate and lead citrate, sections were examined on a Jeol JEM-100SX transmission electron microscope at 100 kV.

Gland extraction and GC analyses

The intersegmental membrane between abdominal segments 8 and 9/10 was carefully dissected from females during the 5th and 6th hr of their third scotophase. Fat bodies and other extraneous reproductive and digestive tissues were removed and the cuticular membrane was carefully divided into a dorsal and a ventral portion by cutting horizontally at the level of the lateral apophyses. The two portions were transferred separately into 50 μl 2:1 chloroform:methanol containing 200 ng tridecanyl acetate (13:OAc) as an internal standard in small test tubes. Extraction was conducted at –10°C for 24 hr. Tissues were then removed and base methanolysis was carried out according to Bjostad *et al.* (1987) with slight modifications. Briefly, the extract was dried under a slow stream of N_2 and 0.5M methanolic KOH was added. After 1 hr, the solution was made acidic by the addition of an equal volume of 1N HCl and extracted with hexane. Alcohol moieties in the extract were converted back into their corresponding acetates by treatment with acetyl chloride. Sample analysis was performed on a 30 m StabliWax® capillary column (film thickness 0.25 μm and 0.25 mm I.D.) (Restak, Bellefonte, PA) using N_2 as carrier gas (column head pressure 10 psi) in a HP 5840 gas chromatograph equipped with a flame ionization detector. The column temperature was initially set at 80°C for 1 min and then programmed to rise to 180°C at 7.5°C/min for 20 min. The temperature was then increased to 220°C at 5°C/min. Peak identification was based on direct comparison with the retention times of authentic standards.

RESULT

External morphology

There are 9 distinguishable abdominal segments in the adult female *O. nubilalis*. Segments 1–7 are covered with scales. Terminal segments 8–10 form the ovipositor that normally remains telescoped within the preceding segments. The 8th abdominal segment is shield-like and heavily sclerotized. The ostium bursae opens just posterior to the 8th sternum (Fig. 1). Segments 9 and 10 are fused to form the sclerotized papillae anales that are characterized by numerous short, spine-like microtrichae and long setae on their lateral and posterior surfaces (Fig. 1). The hindgut and the median oviduct open respectively at the anus and oviporus between the two lobes of the papillae anales. Arising laterally from the papillae anales and fused to the intersegmental membrane between abdominal segment 8 and 9/10 is a pair of apophyses that projects anteriad into the hemocoel (Fig. 1). At the place where these apophyses fused to the intersegmental membrane between abdominal segments 8 and 9/10, the entire intersegmental membrane is roughly divided into a dorsal and a ventral half. Muscles from the anterior segments attach to the free ends of the apophyses (Fig. 8). These muscles serve to control the movement of the papillae anales during oviposition and calling.

Adjoining the 8th segment and the papillae anales is the cylindrical intersegmental membrane that is usually held inverted and hidden underneath the 8th abdominal segment. Eversion of the intersegmental membrane between abdominal segments 8 and 9/10 appears to be caused by an increase in hemolymph pressure. Retraction of the intersegmental membrane probably is brought about by a reduction in hemolymph pressure together with the contraction of muscles attached to the apophyses and the mid-ventral region of the intersegmental membrane.

Scanning electron microscopy revealed that the entire

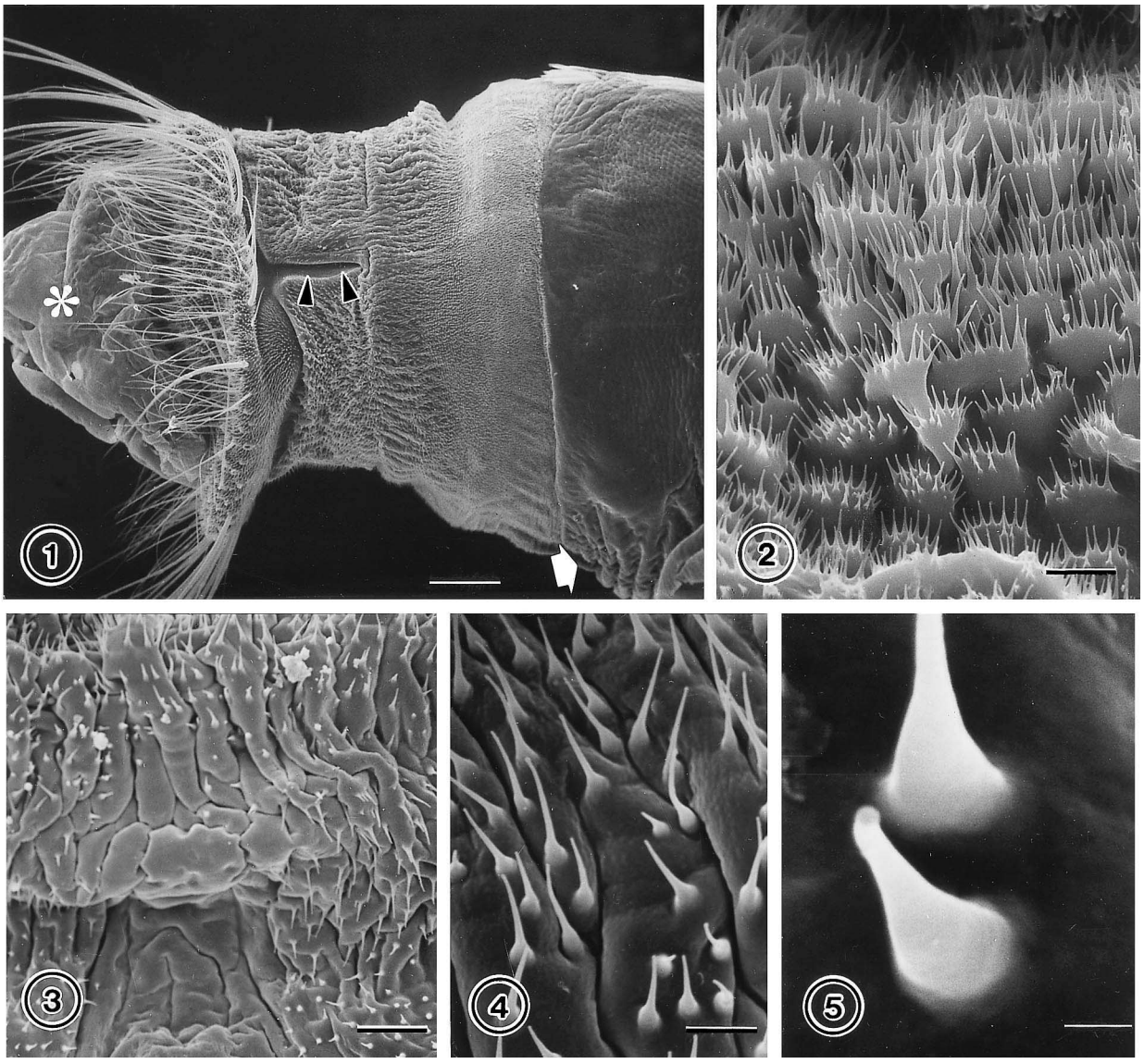

Figs. 1–5. Scanning electron micrographs of the terminal abdominal segments of the female *Ostrinia nubilalis*. **1**). Lateral view of terminal abdominal segments 8–10 showing the intersegmental membrane between abdominal segments 8 and 9/10; note the smooth surface of the heavily sclerotized 8th abdominal segment and the location of the ostium bursae (arrow) and also the papillae annales with the long setae. The cylindrical intersegmental membrane is roughly divided into dorsal and ventral halves by an apophysis (arrowheads). The everted oviduct (asterisk) is an artifact that was introduced during tissue preparation. Scale bar = 100 μm. **2**). Higher magnification of the dorsal region (above the sclerotized rod) of intersegmental membrane between abdominal segments 8 and 9/10; microtrichae are in aggregates of 7–10. Scale bar = 10 μm. **3**) Higher magnification of the ventral region (below the apophysis) of the intersegmental membrane between abdominal segments 8 and 9/10; microtrichae are sparingly located; note the area without microtrichae where several pairs of muscles attach at the hemocoel side. Scale bar = 10 μm. **4**). Microtrichae on the lateral region of the intersegmental membrane between abdominal segments 8 and 9/10. Scale bar = 5 μm. **5**). High magnification of a microtrichae on the dorsal region of the intersegmental membrane between abdominal segments 8 and 9/10. Scale bar = 1 μm.

surface of intersegmental membrane between abdominal segments 8 and 9/10 is wrinkled and decorated with numerous microtrichae (Fig. 1). However, cuticular sculpture varies at different regions of the intersegmental membrane. In the centrodorsal region, the cuticular surface is characterized by the presence of short microtrichia (3–4 μm in length), which often form aggregates of 7–10 (Fig. 2). In contrast, cuticular projections on the rest of the intersegmental membrane are considerably longer (8–20 μm in length) and are distributed evenly on the intersegmental membrane (Figs. 3, 4). Regardles of their location, none of the microtrichia are porous (Fig. 5). The intersegmental membrane anteriad to the ventral tip of the papillae anales is devoid of any cuticular projections (Fig. 3). This demarcates the point of insertion by several pairs of ventral muscles on the hemocoel side of the intersegmental membrane (Fig. 6).

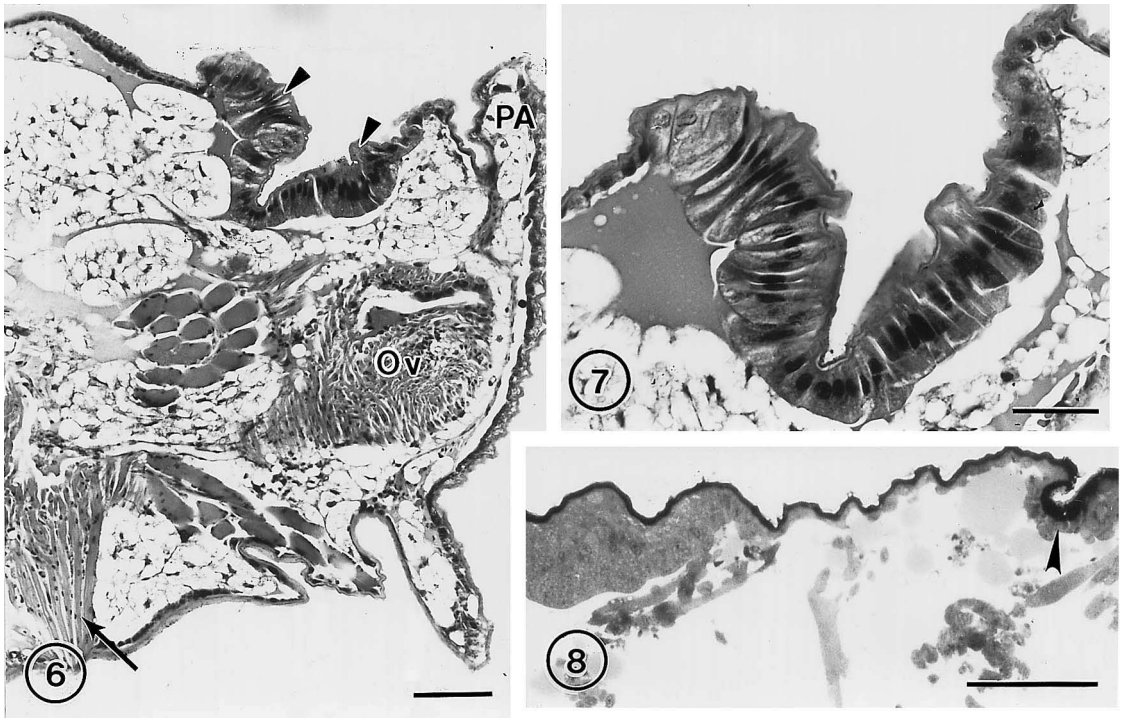

Figs. 6–8. Light micrographs of terminal abdominal segments 8 and 9/10 of *Ostrinia nubilalis*. **6**). Sagittal section through abdominal segments 8–10 showing the position of the hypertrophied epidermal cells (arrowheads) in the centrodorsal region of the intersegmemtal membrane; note point of attachment of muscles at the ventral side of the intersegmental membrane. Ov, oviduct; PA, papillae anales. Scale bar = 100 μm. **7**). Sagittal section through the dorsal region of the intersegmental membrane between abdominal segmental 8 and 9/10 showing the columnar hypertrophied epidermal cells. Scale bar = 50 μm. **8**). Transverse section through the dorsal region of the intersegmental membrane showing the hypertrophied cells. Location of the apophysis is indicated by the arrowhead. Scale bar = 100 μm

Histology

At the dorsal region, the intersegmental membrane between abdominal segments 8 and 9/10 consists of a single layer of hypertrophied columnar epidermal cells. These cells measure 60–100 μm in height (Fig. 7). The dorsal epidermis occupies an area of about 450–500 μm X 350–400 μm at the centrodorsal part of the intersegmental membrane. It is surrounded anteriorly and posteriorly by smaller squamous and cuboidal cells (10–20 μm in height) and laterally by squamous epidermal cells (Figs. 6, 8).

Cuticle

The cuticle consists of a dense outer epicuticle, about 0.5 μm thick, overlying the untanned and lamellated endocuticle, about 1.5–3 μm in thickness (Figs. 9, 10). Each lamella measures 0.25–0.5 μm in thickness. The number of lamellae in the endocuticle, generally ranging from 3–7, varies considerably in different regions of the intersegmental membrane. In most cases, the lamellated appearance of the endocuticle is more distinct in sagittal sections than in transverse sections. In the region where the cuticle is underlined by columnar hypertrophied cells, numerous pore canals transverse the endocuticle in helicoidal fashion to terminate just beneath the dense epicuticle (Fig. 9). These pore canals contain epicuticular filaments measuring 15–20 nm in diameter (Fig. 11). The distribution of pore canals in the ventral cuticle is not as extensive as that in the dorsal cuticle.

In 2-3-day-old females, cuticular lining over the dorsal columnar hypertrophied cells contains numerous spherical lipid droplets, ranging from 0.2 to 1.5 μm in diameter (Fig. 12). These lipid droplets contain a homogeneous electron-lucid substance and, in some cases, they are bounded by a thin layer of electron-dense material (Fig. 12). Lipid droplets are absent in all the cuticular lining of the intersegmental membrane and the dorsal cuticular lining in younger females (Fig. 16).

Dorsal Epidermis

In 2-3-days-old females, the dorsal epidermis is made up of tall columnar cells (80–100 μm in height and 20–30 μm in width) (Fig. 7). The cells rest on a electron-dense basement membrane with a uniform thickness of about 0.2 μm throughout the entire dorsal epidermal region (Fig. 13). The basement membrane apposes closely to the basal plasma membrane of the cells, and there are tracheae interposed between the epidermal cells and the basement membrane (Fig. 13).

Immediately beneath the cuticular lining, the apical plasma membrane is characterized by the formation of tightly packed membrane foldings, measuring 0.3–0.5 μm in depth and 50 nm in width (Fig. 15). At the tips of the apical folds, electron dense material appears as dark plaques

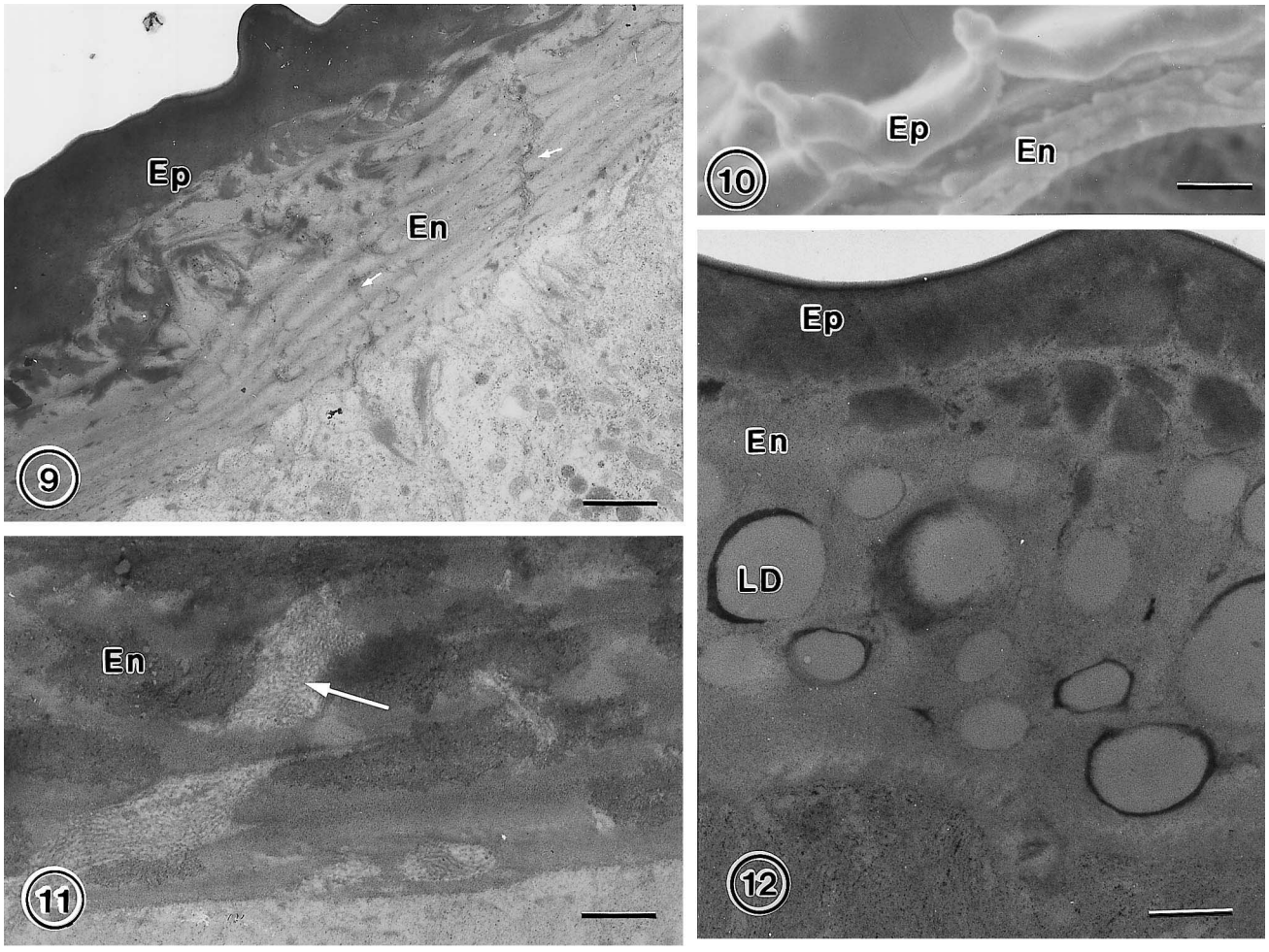

Figs. 9–12. Electron micrographs of the intersegmental membrane between abdominal segments 8 and 9/10 of *Ostrinia nubilalis*. **9**). Apical region of the epidermal cells at the dorsal side of the intersegmental membrane. Numerous pore canals transverse the endocuticle (arrows). En, endocuticle; Ep, epicuticle. Scale bar = 1 μm. **10**). Scanning electron micrograph of the cuticular covering of dorsal intersegmental membrane between abdominal segments 8 and 9/10. The intersegmental membrane was fixed and dehydrated as described in materials and methods and cryofractured under LN_2. Note that only the cuticular covering of the intersegmental membrane is shown because the epidermis was probably lost during the processing. En, endocuticle; Ep, epicuticle. Scale bar = 1 μm. **11**). High magnification of a pore canal showing the epicuticular filaments (arrow). En, endocuticle. Scale bar = 0.5 μm **12**). Cuticular covering of the epidermal cells of the intersegmental membrane between abdominal segments 8 and 9/10 showing the accumulation of lipid droplets (LD) 2-3-days after adult emergence. En, endocuticle; Ep, epicuticle. Scale bar = 0.5 μm.

along the cell-endocuticle interface.

At the apical ends of the cells, plasma membrane of adjacent cells extensively interdigitate (Fig. 15). Desmosomes occur occasionally between neighboring cells along the interdigitated cell membranes. More basal along the lateral margins of the cells, intercellular boundaries are smooth and the cell membranes remain parallel towards the bases of the cells (Fig. 16).

Abundant free ribosomes form the ground cytoplasmic matrix. The most distinct feature in the cytoplasm the spherical lipid droplets (0.5–1.5 μm in diameter) containing a homogeneous electron-lucid material (Fig. 13). Coalescing of small lipid droplets to form larger ones is seen, especially near the apical parts of active glandular cells. Numerous mitochondria with tightly packed cristae and an electron-dense matrix are scattered throughout the cytoplasm (Fig. 14). They exist in a variety of shapes, ranging from sausage-shaped to long branched forms. Close associations of mitochondria with the lipid droplets occur frequently in the cytoplasm (Fig. 14). The cytoplasm also contains a rich array of microtubules, with diameters of about 30 nm, oriented parallel to the long axis of the cell (Fig. 15). Golgi complexes and rough endoplasmic reticulum are infrequent. Smooth endoplasmic reticulum in the form of vesicles, though not very well developed, is found scattered sparingly in the cytoplasm (Fig. 19). The oval or slightly lobulated nucleus occupies the central portion of the cell.

In pharate and young adult females (within 4 hr of adult eclosion), the dorsal epidermis is strikingly different in morphology to that in older females (Fig. 16). The columnar epidermal cells at this stage are much smaller (35–40 μm in depth and 5–10 μm in width). Sandwiched between the cuti-

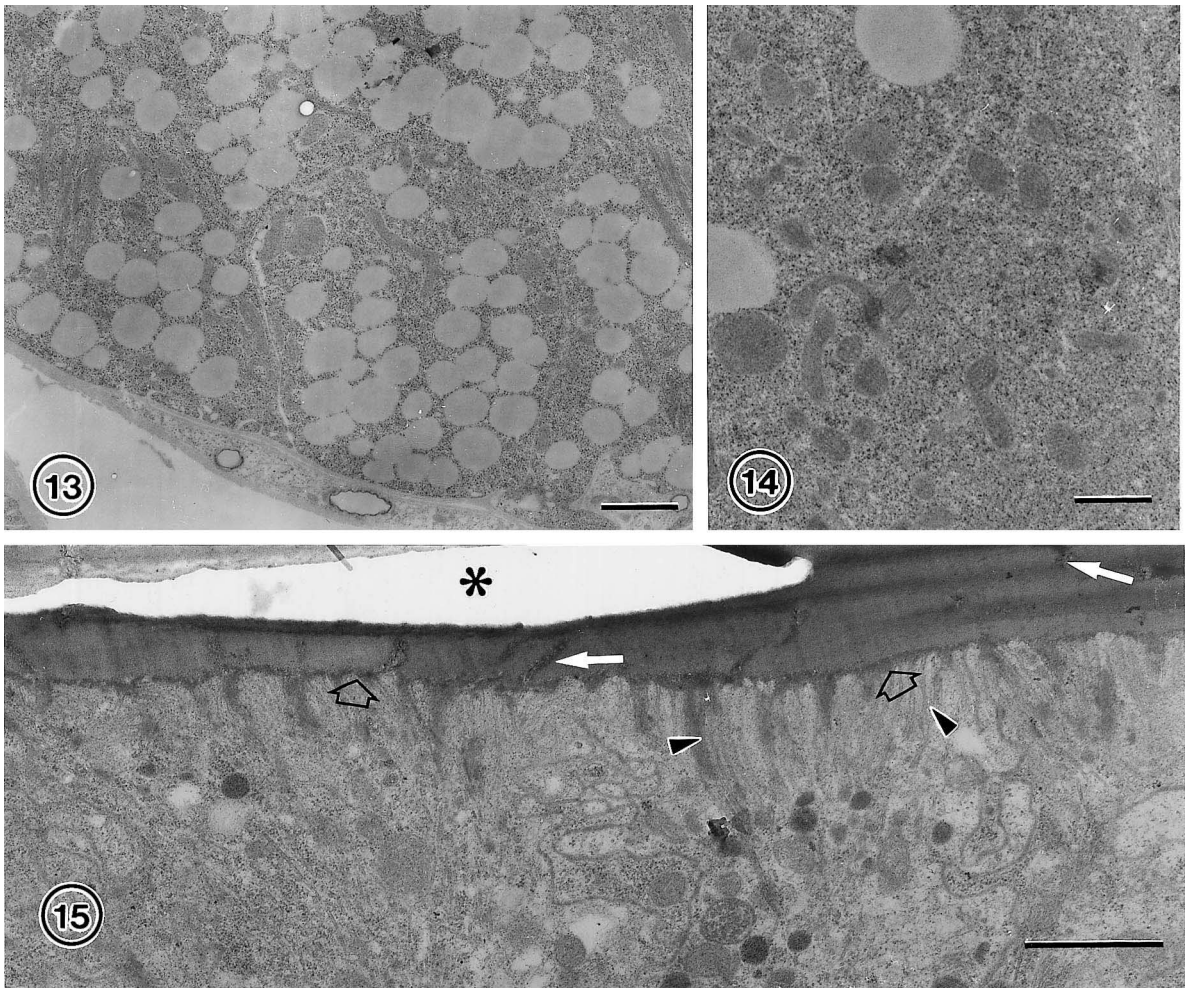

Figs. 13–15. Transmission electron micrographs of epidermal cells at the dorsal intersegmental membrane of abdominal segment 8 and 9/10 of *Ostrinia nubilalis*. **13**) Fully developed adult (2-3-day old) epidermal cells of the dorsal region of the intersegmental membrane between abdominal segments 8 and 9/10. Note numerous lipid droplets present in the cytoplasm. Scale bar = 0.5 μm. **14**) Numerous free ribosomes and mitochondria form the matrix of the cytoplasm of the epidermal cells. Some of the mitochondria are closely associated with the lipid droplets (arrow). Scale bar = 0.6 μm. **15**) Apical region of hypertrophied epidermal cells showing the tightly packed membrane foldings (arrowheads). Note electron-dense plaques accumulate at the tips of the membrane foldings (open arrows) and numerous pore canals transverse the cuticular covering (white arrow). The space in the cuticle (asterisk) is an artifact. Scale bar = 0.8 μm.

cle and the apical plasma membrane is a granular amorphous matrix (Fig. 16). The apical plasma membrane folds are not as elaborated as that seen in 2-3-day-old females (Figs. 15, 16). The lateral plasma membranes are highly convoluted throughout the length of the cell (Fig. 17). Basally, the plasma membrane exhibits extensive invaginations while remaining closely apposed to the basement membrane. The cytoplasmic matrix contains fewer free ribosomes, microtubules and mitochondria. The latter are usually globular or in the form of short rods. Furthermore, lipid droplets, Golgi complexes and smooth and rough endoplasmic reticula are absent. The oval nuclei, however, resemble those in older dorsal epidermal cells (Fig. 16).

Ventral Epidermis

The ventral epidermis is composed of simple cuboidal and squamous cells (Fig. 18). These cells vary considerably in size in different regions of the intersegmental membrane. The cuboidal cells (about 10 μm in height and 8 μm in width) are located anteriad and posteriad to the dorsal epidermis and also along the basal region of the intersegmental membrane (Fig. 6). The squamous cells, on the other hand, generally occur lateral to the dorsal epidermis and they measure 6–8 μm in height and 10–12 μm in width (Fig. 8). These epidermal cells rest on a thin basement membrane, about 50 nm thick. Intercellular boundaries of these epidermal cells, especially those of the squamous epidermis, are highly convoluted. Although apical infoldings are present in these cells, they are loosely formed and poorly organized (Fig. 18). An amorphous matrix similar the one seen in dorsal epidermal cells in younger females often occur between the cells and the cuticular lining (Fig. 18).

Despite the differences in size and shape, both cuboidal and squamous epidermal cells share similar cytological

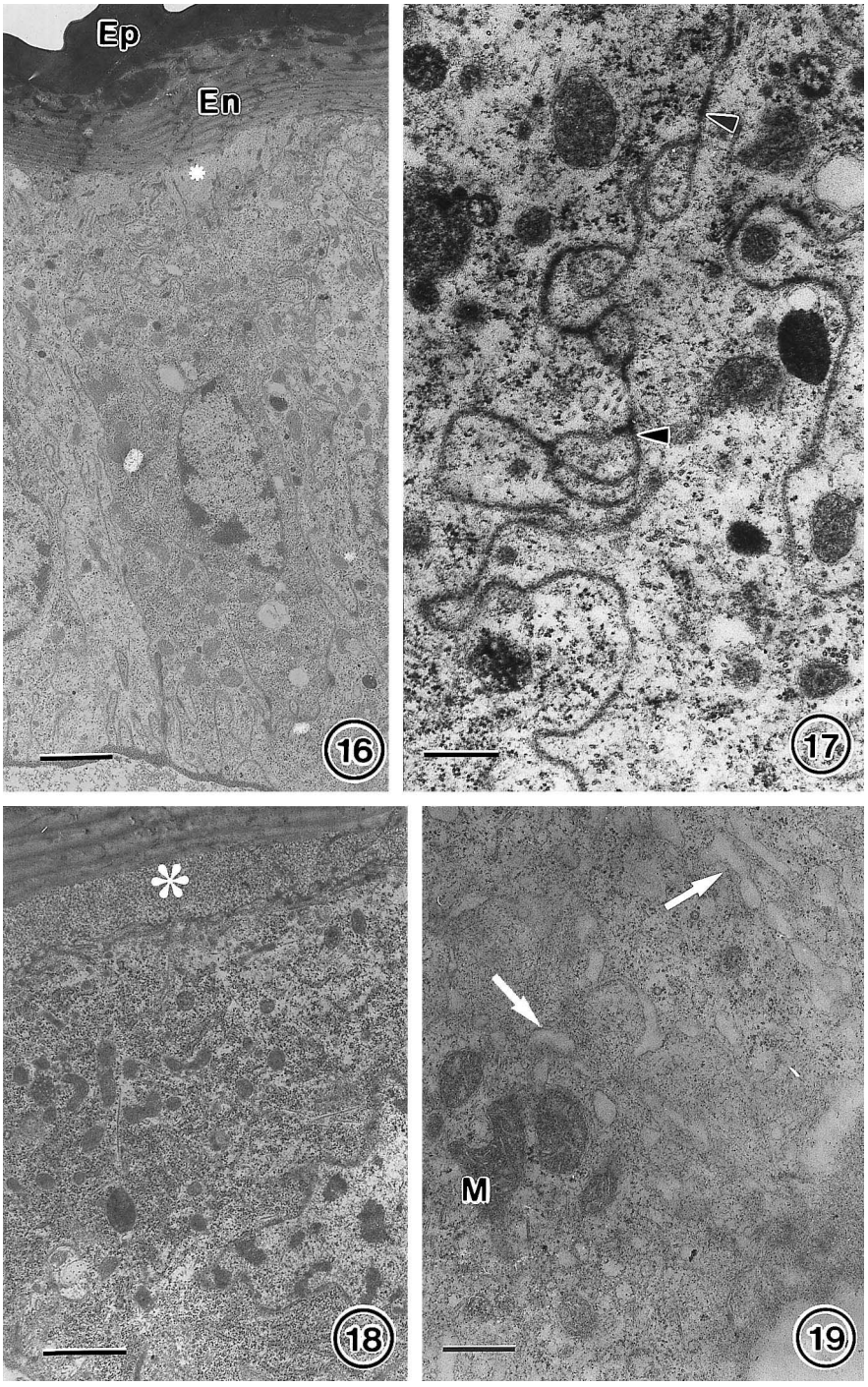

Figs. 16–19. Transmission electron micrographs of epidermal cells at the intersegmental membrane between abdominal segments 8 and 9/10. **16**) Epidermal cells of the dorsal region of the intersegmental membrane between abdominal segments 8 and 9/10 in young females. The cells are much smaller than the epidermal cells found in older females. Microvilli at the apical membrane are not very well developed. Sandwiched between the apical region of the epidermal cells and the cuticular covering is a granular amorphous matrix (asterisk). En endocuticle; Ep = epicuticle. Scale bar = 3.6 μm. **17**) Epidermal cells of the dorsal region of the intersegmental membrane between abdominal segments 8 and 9/10 in young females. The lateral cell membrane is characterized by extensive interdigitations, numerous desmosomes between the cell boundaries (arrowheads). Scale bar = 0.4 μm. **18**) Epidermal cells lining the ventral region of the intersegmental membrane. The cells are cuboidal to squamous and the microvilli at the apical cell membrane is not well developed; an amorphous matrix normally present between the cells and the cuticular covering (asterisk). Scale bar = 1 μm. **19**) Numerous smooth endoplasmic reticula (arrows) in the form of vesicles usually present in the cytoplasm of epidermal cells at the dorsal region of the intersegmental membrane. M, mitochondria. Scale bar = 0.5 μm.

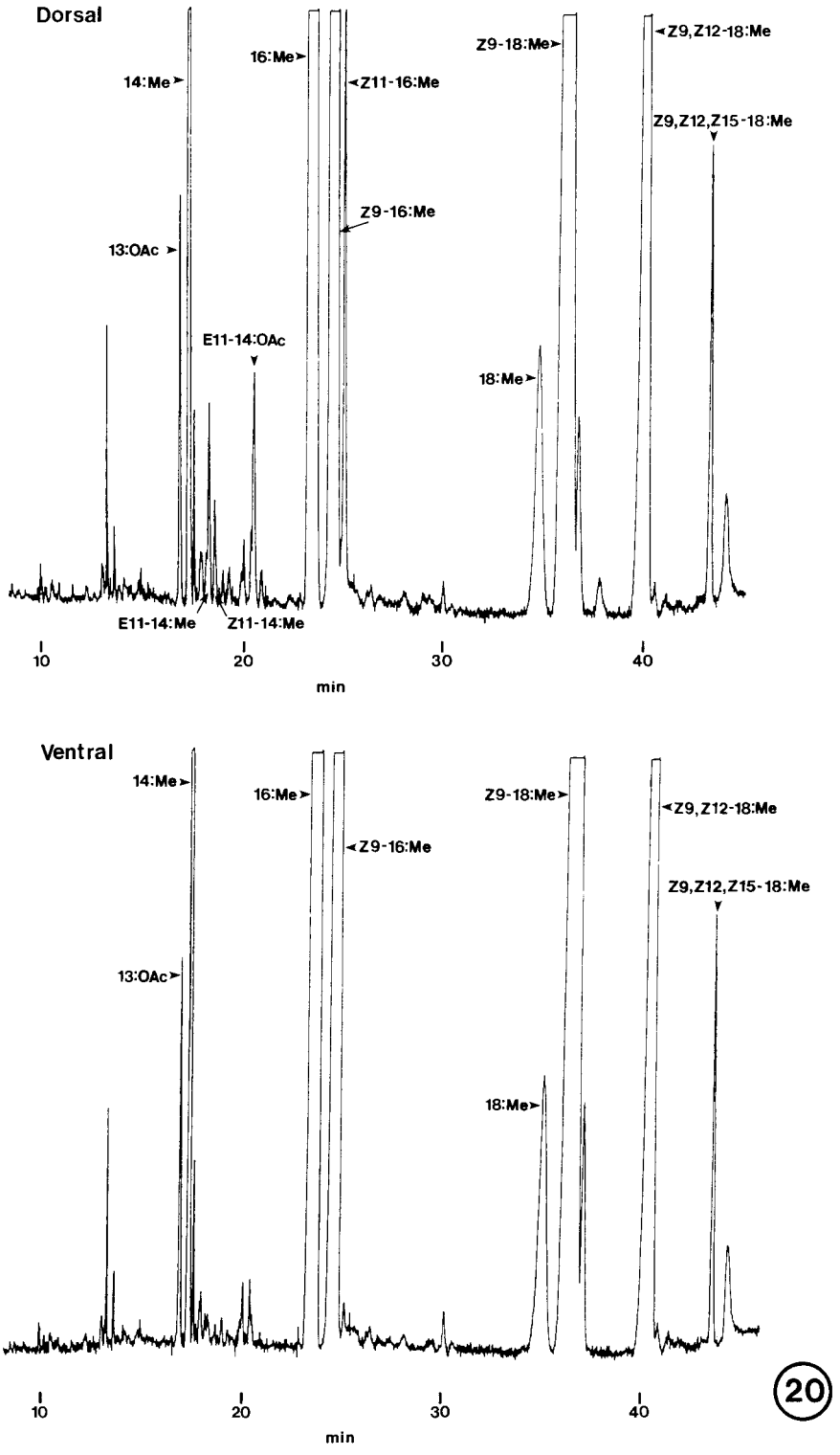

Fig. 20. Gas chromatogram of base methanolysed and acetyl chloride-treated chloroform/methanol extracts of the dorsal and ventral portions of the intersegmental membrane between abdominal segments 8 and 9/10 of *Ostrinia nubilalis*. Equal amounts of the final extracts from the dorsal and ventral intersegmental membrane were injected into the gas chromatograph for comparison. Note the absence of E11-14:OAc, Z/E11-14:Me and Z11-16:Me in the ventral portion of the intersegmental membrane. The amount of the internal standard, 13:OAc, shown on both tracings correspond to 200 ng. Refer to text for a full description of the abbreviations.

characteristics. The cytoplasm contains a moderate number of mitochondria of various sizes and shapes. Ribosomes, unattached or in small aggregates, are randomly dispersed in the cytoplasm. Short lengths of rough endoplasmic reticulum and vesicular smooth endoplasmic reticulum are sometimes encountered in the cytoplasm and other organized membrane structures are rare. Lipid droplets are lacking in any of the sections examined. Nuclei are round in cuboidal epidermal cells whereas the squamous cells contain slightly lobulated nuclei.

Fatty Acids Analysis

Gas chromatographic analysis of base methanolysed and acetyl chloride-treated chloroform/methanol extracts of the intersegmental membrane reveals the presence of the sex pheromone components, E11-14:OAc and its immediate fatty acyl precursors, methyl *(Z)*-11- and methyl *(E)*-11- tetradecenoate (Z11- and E11-14:Me) only in the dorsal intersegmental membrane (Fig. 20), and no detectable amounts in the ventral intersegmental membrane. Both dorsal and ventral halves of the intersegmental membrane contain large amounts of the common acids, methyl tetradecanoate (14:Me), methyl hexadecanoate (16:Me), methyl *(Z)*- 9-hexadecenoate (Z9-16:Me), methyl octadecanoate (18:Me), methyl *(Z)*- 9-octadecenoate (Z9-18:Me), methyl *(Z,Z)*- 9,12-octadecadienoate (Z9,Z12-18:Me) and methyl *(Z,Z,Z)*- 9,12,15-octadecatrienoate (Z9,Z12,Z15-18:Me). The dorsal intersegmental membrane contains a large amount of methyl *(Z)*-11-hexadecenoate (Z11-16:Me), which could not be detected in its ventral counterpart.

DISCUSSION

Present histological examinations of the terminal abdominal segments of female *O. nubilalis* indicate that only the centrodorsal part of the intersegmental membrane is lined with hypertrophied cells. Ultrastructural observations showed that these epidermal cells possess the general cytological features commonly found in sex pheromone-producing-gland cells in other lepidopteran insects (Percy-Cunningham and MacDonald 1987). These features include the presence of numerous mitochondria, lipid droplets both in the cell and the overlying cuticle, and also development of apical plasma membrane foldings. Such characteristic features are either absent or not well defined in epidermal cells occurring elsewhere in the intersegmental membrane and in other parts of the terminal abdominal segments. Furthermore, the major sex pheromone components, E11-14:OAc, and its immediate fatty acyl precursors, Z/E11-14:Me, are detected only at the dorsal portion of the intersegmental membrane. The latter observation also suggests the presence of a Δ11-desaturase, which is the key enzyme involved in the biosynthesis of sex pheromones in many lepidopterous insects (Bjostad *et al.* 1987), only in the dorsal part of the intersegmental membrane. Thus, morphological and biochemical observations in the present study strongly indicate that the sex pheromone gland of female *O. nubilalis* is not a ring gland as previous shown (Hammad 1961), but rather a dorsal scent fold (Götz 1951).

Ultrastructural studies of sex pheromone glands of various species of female Lepidoptera have established that the presence of smooth endoplasmic reticulum is a common morphological feature of the modified glandular cells (Percy-Cunningham and MacDonald 1987). In *O. nubilalis*, only a few smooth endoplasmic reticulum occur in the active pheromone gland cell. Similar situation was also observed in the silkworm moth, *Bombyx mori* L. (Bombycidae) (Waku and Sumimoto 1969). The absence of well-developed smooth endoplasmic reticulum in *O. nubilalis* pheromone gland cells may be a fixation artifact introduced during tissue preparation. In vertebrates such as rat liver cells, distribution and quantity of vesicular type smooth endoplasmic reticulum have been found to undergo extensive diurnal changes (Chedid and Nair 1972). Recently, *Fonagy et al*. (2001) conducted a study to correlate the changes in cytoplasmic lipid droplets in the pheromone-producing cells of the silkmoth, *B. mori*, and they showed a daily fluctuation in size and number of lipid droplets during the photophase. In the present study, tissues were obtained from insects 4, 24, and 48 hr after adult eclosion (all within 2 hr of the end of the scotophase). If there is a diurnal change in the amount of smooth endoplasmic reticulum in the pheromone gland cell, the period when the cell exhibits a full development of smooth endoplasmic reticulum may have been missed in the current study.

Although there is an indication that the accumulation of lipid in the pheromone glands of *O. nubilalis* and other moths correlates with the amount of extractable pheromone from the gland (Waku and Sumimoto 1969; Feng and Roelofs 1977; Percy 1979; Ma and Roelofs unpublished observations), the role of lipid deposits in the pheromone gland cells and in the overlying cuticle in *O. nubilalis* and other lepidopterous insects is not fully understood (Bjostad *et al.* 1987). The assumption that this lipid deposits may act as a form of storage of sex pheromone available for immediate secretion, however is based solely on morphological observations and lacks the support of biochemical evidence. In the tortricid moth *Argyrotaenia velutinana* and in *O. nubilalis*, the triacylglycerols constitute the main pool of non-membrane-origin lipid, which represents the contents of these lipid spheres (Bjostad *et al*. 1987; Ma and Roelofs unpublished observations). A large amount of the immediate acyl precursors involved in sex pheromone biosynthesis occurs as triacylglycerols (Bjostad *et al.* 1987). However, fatty acids mass-labeled with stable isotopes in synthetic triacylglycerols were not incorporated into the sex pheromone components of *A. velutinana* (Bjostad and Roelofs 1986). These authors suggested that this lipid class is not a donor of the immediate fatty acyl precursors for pheromone biosynthesis, but instead acts as a “dumping ground” for fatty acids that are not used in pheromone biosynthesis. Hence, the physiological role of lipid deposits in the sex pheromone

gland of Lepidoptera requires further clarification.

The cuticle overlying the dorsal epidermis apparently contains more pore canals than does the cuticular covering of epidermis elsewhere on the intersegmental membrane. These pore canals usually contain epicuticular filaments and the latter have been implicated as structures involved in the translocation of the secreted pheromone through the cuticular lining to the exterior (Percy 1974; 1979). A recent study on the sex pheromone gland of *Helicoverpa zea* by Raina *et al*. (2000) using low temperature scanning electron microscope have shown the presence of excreted droplets at the tip of cuticular hair on the pheromone gland. These authors also showed the presence of pore canals in the epicuticle (Raina *et al.* 2000). In *O. nubilalis*, pore canals were not seen to penetrate the tanned epicuticle and pores were not observed on the external surface of the cuticle. Perhaps more vigorous tissue preparation procedures are required to reveal these structures in *O. nubilalis*.

The functional role of numerous microtubules found in *O. nubilalis* pheromone gland cells also is not clear. Microtubules have been reported to be important in providing mechanical support for midge follicles (Tucker and Meats 1976; Went 1978). In the hemipteran bug, *Rhodnius prolixus* Stal, (Reduviidae), microtubules are an important cytological element that is involved in the change of the follicular epithelium during vitellogenesis (Huebner 1976; Abu-Hakima and Davey 1977). The periodic folding and unfolding of the modified membrane during the female's calling activity may impose an extreme mechanical stress on the hypertrophied pheromone gland cells. The microtubules in this case may act as a cytoskeletal system that provides a direct strengthening role for maintaining the structural integrity of the hypertrophied cells.

In summary, current morphological observations and biochemical studies confirmed that the sex pheromone glandular epidermis in *O. nubilalis* female is located only in the dorsal part of the intersegmental membrane between abdominal segments 8 and 9/10. The modified epidermal cells undergo drastic morphological changes to mature into active glandular cells. The hypertrophied glandular cells exhibit the cytological characteristics found in other lepidopteran pheromone gland cells. Such morphological features are poorly represented in epidermal cells found elsewhere on the intersegmental membrane.

ACKNOWLEDGEMENTS

We thank Mary Lou Hessney for rearing the insects used in this study. This research was supported in part by a National Science Foundation Grant No. DBC-9017793 to W.L.R. This is publication No. J9995 of Mississippi Agricultural and Forestry Experiment Station

REFERENCES

Abu-Hakima R, Davey KG (1977) The action of juvenile hormone on the follicle cells of *Rhodnius prolixus in vitro*: The effect of colchicine and cytochalasin B. Gen Comp Endocrinol. 32: 360–370

Bjostad LB, Roelofs WL (1986) Sex pheromone biosynthesis in the redbanded leafroller moth, studied by mass-labeling with stabled isotopes and analysis with mass spectrometry. J Chem Ecol 12: 431–450

Bjostad LB, Wolf WA, Roelofs WL (1987) Pheromone biosynthesis in lepidopterans: Denaturation and chain shortening. In "Pheromone biochemistry" Ed by GD prestwich, GJ Bloomquist, Academic Press, New York

Carrow GM, Calabrese RL, Williams CM (1981) Spontaneous and evoked release of prothoracicotropin from multiple neurohemal organs of the tobacco hornworm. Proc Natl Acad Sci USA 78: 5866–5870

Chedid A, Nair V (1972) Diurnal rhythm in endoplasmic reticulum of rat liver: Electron microscopic study. Science 175: 176–179

Chow YS, Chen J, Lin-Chow SH (1976) Anatomy of the female sex pheromone gland of the diamondback moth, *Plutella xylostella* (L.) (Lepidoptera: Plutellidae). Int J Insect Morphol Embryol 5: 197–203

Feng KC, Roelofs WL (1977) Sex pheromone gland development in redbanded leafroller moth, *Argyrotaenia velutinana*, pupae and adults. Ann Ent Soc Am 70: 721–732

Fonagy A, Yokoyama N, Matsumoto S (2001) Physiological status and change of cytoplasmic lipid droplets in the pheromone-producing cells of the silkmoth, *Bombyx mori*. Arthro Str Devel 30: 113–123

Glover TJ, Tang XH, Roelofs WL (1987) Sex pheromone blend discrimination by male moths from *E* and *Z* strains of European corn borer. J Chem Ecol 13: 143–151

Götz B (1951) Die sexualduftstoffe an Lepidopteren. Experientia 7: 406–418

Hammad SM (1961) The morphology and histology of the sexual scent glands in certain female lepidopterous moths. Bull Soc ent Egypte 45: 471–482

Huebner E (1976) Experimental modulation of the follicular epithelium in *Rhodnius* oocytes by juvenile hormone and other agents. J Cell Biol 70: 251a

Klun JA (1968) Isolation of a sex pheromone of the European corn borer. J Econ Entomol 61: 484–485

Klun JA, Junk GA (1970) *cis* -11-Tetradecenyl acetate, a sex stimulant of the European corn borer. J Econ Entomol 63: 779–780

Kochansky J, Cardé RT, Liebherr J, and Roelofs WL (1975) Sex pheromone of the European corn borer, *Ostrinia nubilalis* (Lepidoptera: Pyralidae), in New York. J Chem Ecol 1: 225–231

Ma PWK, Roelofs WL (1995) Sites of synthesis and release of PBAN-like factor in female European corn borer, *Ostrinia nubilalis*. J Insect Physiol. 41: 339–350

Percy J (1979) Development and ultrastructure of sex-pheromone gland cells in females of the cabbage looper moth, *Trichoplusia ni* (Hübner) (Lepidoptera: Noctuidae). Can J Zool 57: 220–236

Percy-Cunningham JE, MacDonald JA (1987) Biology and ultrastructure of sex pheromone-producing glands. In "Pheromone biochemistry" Ed by GD prestwich, GJ Blomquist, Academic Press, Orlando

Raina AK, Wergin WP, Murphy CA Erbe EF (2000) Structural organization of the sex pheromone gland in *Helicoverpa zea* in relation to pheromone production and release. Arthro Str Devel 29: 343–353

Sreng I, Sreng L (1988) Fine structure of the female sex pheromone-producing glands in *Sesamia nonagrioides* Lef. (Lepidoptera: Noctuidae). Int J Insect Morphol and Embryol 17: 345–357

Teal PEA, Carsyle TC Tumlinson JH (1983) Epidermal glands in terminal abdominal segments of female *Heliothis virescens* (F.) (Lepidoptera: Noctuidae). Ann Ent Soc Am 76: 242–247

Tucker JB Meats M (1976) Microtubules and control of insect egg shape. J Cell Biol 71: 207–217

Waku Y, Sumimoto K (1969) Ultrastructure and secretory mechanism of the alluring gland cell in the silkworm, *Bombyx mori* L. (Lepidoptera: Bombycidae). Appl Ent Zool 4: 135–146

Went DF (1978) Oocyte maturation without follicular epithelium alters egg shape in a dipteran species. J Exp Zool 205: 149–155

(Received November 14, 2001 / Accepeted February 23, 2002)